MedCrave
Step into the World of Research

MOJ Polymer Science

Research Article

Open Access

CrossMark

Synthesis and characterization of Ni and Cu doped Zno

Abstract

In this work pure and transition elements (Ni & Cu) doped Zinc Oxide is prepared. All the samples were prepared through chemical co-precipitation method, by using sulfates of metallic precursors. We have doped pure ZnO with Ni and Cu by 3% by weight concentration. Further the structural, Crystallite size and band gap approximation studies were performed by utilizing X-ray diffraction and spectroscopic techniques respectively. X-ray diffraction (XRD) result indicates that the sample possess a crystalline wurtzite single phase. Crystallite size is in 19-30nm range. PL characterization gives optical band gap that is 2.65eV-3.02eV. FTIR gives the molecular band present in the samples. UV-Vis shows red shift in peak wavelength.

Keywords: nanoparticles, single crystal, pyroelectric properties, acoustic wave resonator, piezoelectricity, absorption, zinc oxide, white pigments, muffle furnace, ITO, AFM, UV-Vis absorption spectroscopy, nanocomposites

Volume 1 Issue 1 - 2017

Jyotsna Chauhan, Neelmani Shrivastav, Ashish Dugaya, Devendra Pandey
Department of Nanotechnology, Rajiv Gandhi Technical University, India

Correspondence: Jyotsna Chauhan, Department of Nanotechnology, Rajiv Gandhi Technical University, Bhopal, India, Email jyotsnachauhan2006@gmail.com

Received: January 30, 2017 | **Published:** April 11, 2017

Abbreviations: XRD, X-ray diffraction; ZNO, zinc oxide; FWHM, full width at the half maximum; AFM, atomic force microscope; eV, electronvolt; FTIR, fourier transform infrared spectroscopy; UV Vis, ultraviolet visible spectroscopy

Introduction

Valued for ZnO ultra violet absorbance, wide chemistry, piezoelectricity and luminescence at high temperatures, ZnO has penetrated far into industry, and is one of the critical buildings in today modern society.[1] ZnO is indeed a key element in many industrial manufacturing processes including paints, cosmetics, pharmaceuticals, plastic, batteries, electrical equipment, rubber, soap, textile, floor covering etc. with improvement in growth technology of ZnO nanostructures, single crystal and nanoparticles, ZnO devices will become increasing functional in the near future.[2] Metal oxide nanoparticles were extensively investigated due to their applications in the field of spintronics,[3] photoelectronic,[4] sensor,[5] lasing devices[6] and light emitting diodes,[7] etc. The properties of these nano materials incredibly altered due to quantum confinement and enhanced surface to volume ratio.[8] ZnO is a multifunctional material.[9] The piezoelectric and pyroelectric properties of ZnO mean that it can be used as a sensor, converter, energy generator and photo catalyst in hydrogen production.[10] The physical and chemical properties of ZnO nano materials can be easily tailored as per the demand of device fabrication

Properties

ZnO is a relatively very soft material with approximate hardness just 4.5. Its elastic constants are relatively smaller than those of other III-V semiconductors, e.g. GaN. The high heat capacity and high heat conductivity, low values of thermal expansion and high melting points are 11 some of the characteristics of ZnO. Among the semiconductors bonded tetrahedrally, ZnO has the highest piezoelectric tensor. This makes it an important material for many piezoelectric applications, which require a high degree of electromechanical coupling among them. Piezoelectricity of ZnO has been extensively studied for various applications in force sensing, acoustic wave resonator, acousto-optic modulator, etc.[11]

ZnO has a quite large band gap of 3.3eV at room temperature and 60meV excitation energy,[12] The advantages of a large band gap include higher values of breakdown voltages, sustaining large electric fields, high-temperature and high-power operations. ZnO has n-type character, in the absence of doping. Non-stoichiometry is usually the origin of n-type character. Due to defects such as oxygen vacancies and zinc interstitials, P-type and n-type ZnO nano wires can serve as p-n junction diodes and light emitting diodes. Zinc oxide is generally transparent to visible light but strongly absorbs ultra violet light below 365.5nm many papers show its optical properties. The absorption in ZnO is stronger than other white pigments. In the region of visible wavelengths, regular zinc oxide appears white, but, retile and anatase titanium dioxide have a higher reactive index and thus has a superior opacity.[13]

The band gap energy (between valence and conducting bands) is 3.2eV. Under ultra violet light zinc oxide is photoconductive. The combination of optical and semiconductor properties of doped Zinc oxide make a contender for new generations of devices. absorption of solar radiation in photovoltaic cells is much higher in materials composed of nanoparticles than it is in thin films of continuous sheets of material it means that they increase the efficiency, the smaller the particles, the greater the solar absorption.[14]

Experimental work

Several eminent research groups were studied and analyzed that metal-modified oxide semiconductor material have the potential to act and used as catalysts, sensors, substrates for surface-enhance Raman scattering and colloidal entities with unique optical properties.[15] For synthesis of the ZnO nanoparticles first we have to take two materials that are precursor one is of zinc precursor and other is of Oxygen.[16] For synthesis of the Ni doped ZnO Zinc Sulfate and Nickel sulfate and NaOH were used, and for Cu doped ZnO Copper chloride, Zinc chloride and NaOH were used. When the particle growth is started and they are starting to form, a capping agent must be added that stop further growth of the particle.

We were used Ethylene Glycol as capping agent. Analytical

grade materials were used for the synthesis of ZnO: Ni and ZnO: Cu nanoparticles. [$ZnSO_4 \cdot 7H_2O$] (0.2 M), [$NiSO_4.6H_2O$] (0.2M) and NaOH (1M) are used as the starting material for the synthesis of Ni doped zinc oxide nanoparticles. We have doped the Ni and Cu in the ZnO both with 3% by weight. So we have used Zinc Chloride 97% and 3% Nickel sulphate and Copper chloride. First we have weighting the starting material according to their molarities in the solution.

$ZnSO_4 \cdot 7H_2O$ and $NiSO_4.6H_2O$ were dissolved in 30ml distilled water under stirring at room temperature for 30 min both solutions were prepared separately. Then these solutions are mixed during continuously stirring, an aqueous solution of NaOH was slowly added to the mixture under constant stirring until the pH of the solution reached to 10. During adding of NaOH solution, precipitation was start. After adding of NaOH, 10ml EG was added immediately. The final solution was then stirred for 20 hours at room temperature, so that homogeneity can be maintained. The reaction mixture was centrifuged to get the precipitate out, before the washing of sample pH was above the 10 then samples was washed several times until the pH was 7. After washing we have dried sample at 150°C. The sample thus obtained in the powder form to make fine particles we have grinded it and then it was calcined at 500°C for 4h in the muffle furnace (Figure 1).

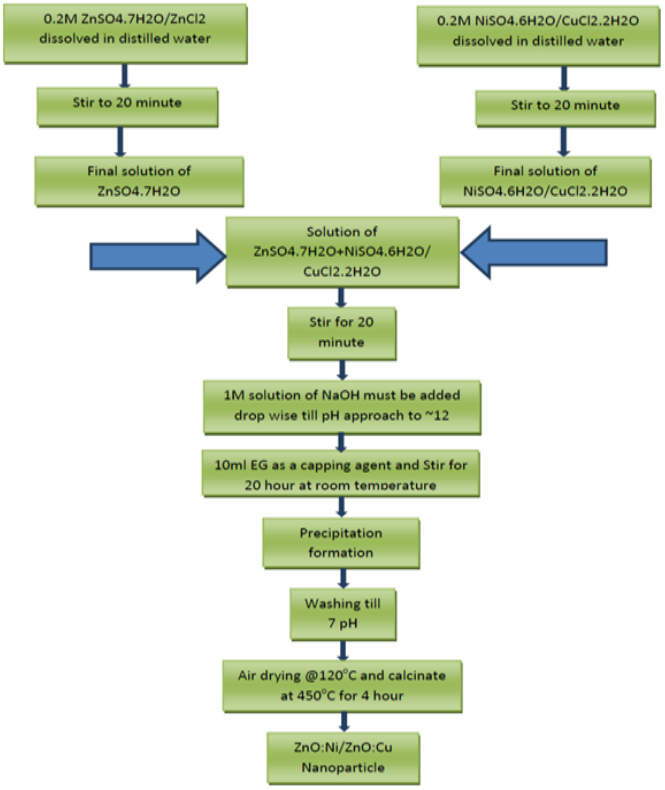

Figure 1 Flow chart of experimental work.

Chemical equation

a) $ZnSO_4.7H_2O + NiSO_4.6H_2O + 2NaOH \quad ZnNiO + 2Na + 2SO_4 + 14H_2O$

b) $ZnCl_2 + CuCl_2*2H_2O + 2NaOH \quad ZnCuO + 2Na + 4Cl + 3H_2O$

Result and discussion

X-ray diffraction study (XRD)

X-ray diffraction study confirms that the synthesized material was ZnO with wurtzite phase and the entire diffraction peaks are in agreement with the standard JCPDS data (card No.36-1451). The X-ray diffraction data were recorded by using Cu Kα radiation (λ=1.5406A°). The average grain size was calculated with the help of Scherrer equation using the FWHM of all peaks. Most importantly, all of the XRD peaks were attributed to ZnO and no other undesired peaks were observed due to secondary phases or impurity phases within the detection limit of the X-ray diffractometer.[17]

Grain size calculation

Scherrer equation is

$$D = 0.89\lambda/(\beta \cos\theta) \quad \ldots\ldots\ldots\ldots\ldots\ldots\ldots\ldots (2)$$

Where D is the grain size, λ is the wavelength of x-ray radiation, β is the full width at the half maximum (FWHM) of the ZnO and θ is the diffraction angle. Figure 2 shows first three peaks of undoped ZnO, Ni doped ZnO and Cu doped ZnO. The FWHM is required for calculation of grain size by Debye Scherrer equation. I have calculate FWHM with the help of origin program, first I have expand the XRD pattern by rescale the pattern around any one peak at which FWHM calculation required. Then by using the screen reader tool measure the maximum intensity of the peak. By the name β is the width of the peak at half of the peak intensity so that we calculate X1 and X2 value of peak at the half of maximum intensity and the difference between the X1 and X2 gives us FWHM of that peak. β has a relation with the grain size, as we seen in the standard JCPDS data, which is pattern of bulk material (that is very large in size) only a line is shown at the peak position it means FWHM of peak of JCPDS data is minimum or near to zero. But as the size of grain is decrease FWHM is increase so that it is clear that FWHM is inversely proportional to the grain size of the material (Figure 3).

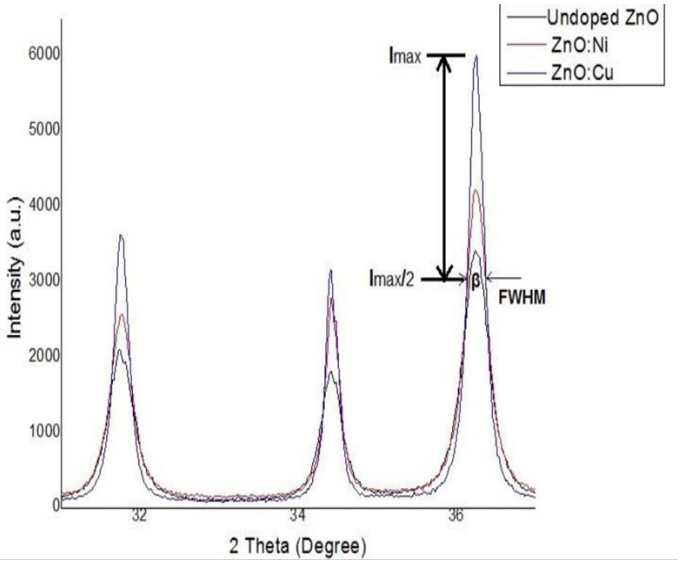

Figure 2: Comparative XRD Pattern of undoped, Ni and Cu doped ZnO.

Citation: Chauhan J, Shrivastav N, Dugaya A, et al. Synthesis and characterization of Ni and Cu doped Zno. *MOJ Poly Sci.* 2017;1(1):26–34.
DOI: 10.15406/mojps.2017.01.00005

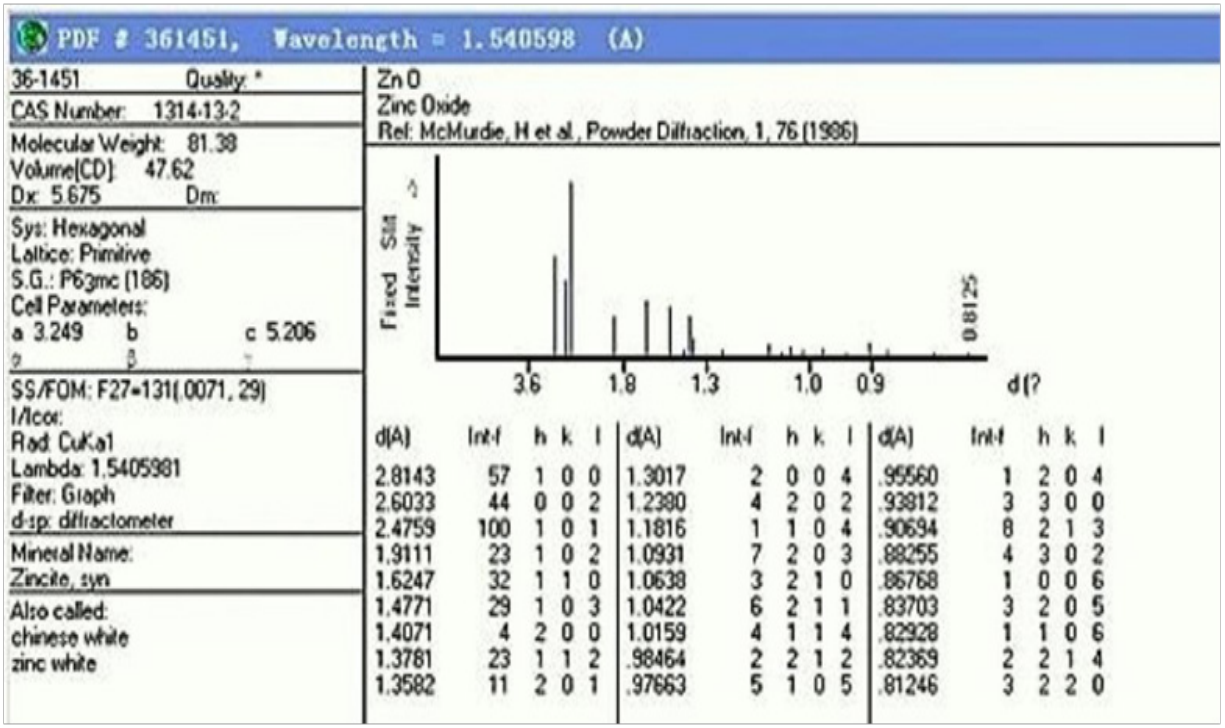

Figure 3 XRD reference data for ZnO wurtzite JCPDS.

Un doped ZnO XRD

The peak positions in the Figure 4 indicate the formation of hexagonal wurtzite crystal structure with three most preferred orientations (1 0 0), (0 0 2) and (1 0 1), which are in very good agreement with the standard JCPDS (N0-36-1451) (Figure 3). These three peaks confirmed that it does not have any secondary phase. From the XRD spectra (Figure 4) it is evident that no characteristic peaks of impurities are obtained. This indicates the absence of impurities in the present nanoparticles. The diffraction peaks obtained are strong and narrow indicating that the nanocrystalline undoped ZnO has good crystallinity. The grain size was estimated using Debye-Scherrer equation (2).

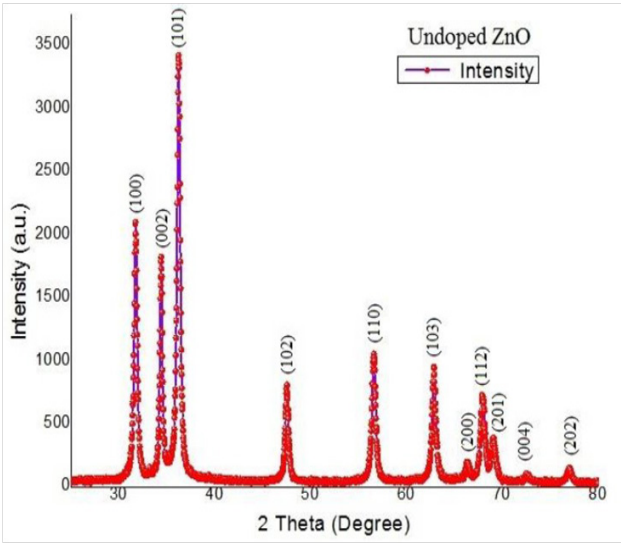

Figure 4 XRD pattern of undoped ZnO.

The inter planar spacing can be calculated from the Bragg's law-

$2d\sin\theta=n\lambda$……. (3).

We have calculated the d value for all the peaks and match it with the standard data given in the literature and it is found that d spacing of our sample is similar with standard value. The average grain size of undoped ZnO is 20nm.

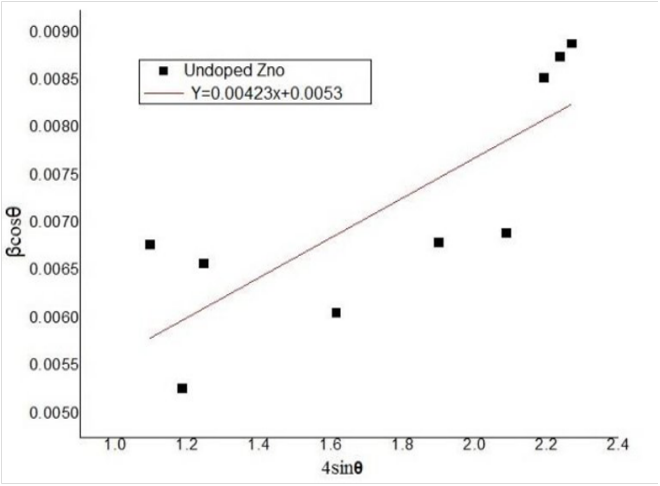

Figure 5 W-H Plot of undoped ZnO.

Strain calculation

Peak broadening may not only come from the size effect, but can also be due to strain in the particles. One way to separate the stress due to particle size from that due to stress is by the Williamson-Hall expression (4) where η is the strain in the particles which is a dimensionless quantity. For non-uniform strain the formula is given below.

Citation: Chauhan J, Shrivastav N, Dugaya A, et al. Synthesis and characterization of Ni and Cu doped Zno. *MOJ Poly Sci.* 2017;1(1):26–34.
DOI: 10.15406/mojps.2017.01.00005

Average strain (ε) calculated by using equation (5)

$\varepsilon=\beta/4\tan\theta$…….. (5)

The average grain size of the Undoped ZnO has been found to be ~20nm. From the Table 1 it is clear that the value of strain is increases when the particle size is decrease. Strain is highest for the lowest particle size; the average strain is 0.004235 that is extracted from the slope of the W-H plot. The Figure 6 is XRD pattern of Ni doped ZnO material this was calcinated at 450°C for 4hr, and it has the highest intensity peak at the angle of 36.236 degree, that is (1 0 1) peak. Peak No. 1, 2 and 3 are (1 0 0), (0 0 2) and (1 0 1) that confirm the structure of the prepared sample. With the XRD pattern we can say that our sample has hexagonal wurtzite structure and it does not have any other diffraction or impurity peaks.

Average grain size of Ni doped ZnO is ~22nm. It was also revealed from the particle size determination that the introduction of the Ni ions into ZnO increases the grain size. The size of the grain of sample is increases by doping Ni. Grain size of this sample is slightly higher than the undoped ZnO. We know that strain is dependent on the size of the particle so that its strain is slightly less than previous sample average strain of Ni doped ZnO is 0.004059 that is comes from slope of W-H plot Figure 7 of ZnO: Ni. d spacing of ZnO: Ni is also different from the Pure ZnO it shows that by the effect of doping.

The Figure 8 shows XRD pattern of copper doped ZnO sample and W-H plot (Figure 9). Copper doped ZnO also has the hexagonal wurtzite structure and successfully matched with the JCPDS (Card No. 36-1451). Peak positions of all three samples are not exactly same there is some difference in the position of the peaks. Above Table 3 shows that average grain size of copper doped ZnO is ~30nm that is larger than both undoped and Ni doped ZnO. When the size is increases strain is reduced strain of copper doped sample is 0.002801 that is lower than strain of undoped and Ni doped sample. All peaks and FWHM of all peaks is used for the calculation. We can also calculate the grain size, average strain and Non uniform strain using the peak that has highest intensity; in our samples Peak (1 0 1) has highest intensity. So I have also calculated corresponding to (1 0 1) peak. Doping of the material in ZnO affect the lattice parameter and it diffuse to the crystal site, both Ni and Cu are replace zinc Site in the ZnO so they are affect lattice parameter and increased the crystallite size.

Table 1 Analysis of XRD of Un doped ZnO

Peak No.	2θ (degree)	hkl	FWHM (β)	Standard d(A°)	Calculated d(A°)	D(nm)	ε
1	31.7477	(100)	0.3899	2.807	2.8151	21.23	0.005964
2	34.4167	(002)	0.3177	2.593	2.6026	26.24	0.004462
3	36.2365	(101)	0.3985	2.469	2.476	21.03	0.005297
4	47.5596	(102)	0.3812	1.905	1.9096	22.83	0.003763
5	56.6181	(110)	0.4447	1.620	1.6236	20.34	0.003591
6	62.866	(103)	0.465	1.472	1.4765	20.07	0.003309
7	66.4044	(200)	0.5863	1.407	1.4061	16.23	0.003897
8	97.9209	(112)	0.6066	1.374	1.3783	15.83	0.003917
9	69.1341	(201)	0.6209	1.354	1.3571	15.57	0.003920
Average						~20nm	0.004235

Table 2 Analysis of XRD of ZnO: Ni

Peak No.	2θ (degree)	hkl	FWHM (β)	d(A°)	D(nm)	ε
1	31.7679	(100)	0.3465	2.8113	23.9	0.005296
2	34.4167	(002)	0.2310	2.6026	36.09	0.003244
3	36.2365	(101)	0.3639	2.4760	24.18	0.004837
4	47.5394	(102)	0.3494	1.9103	24.90	0.003450
5	56.5978	(110)	0.4130	1.6242	21.90	0.003337
6	62.8862	(103)	0.4852	1.476	19.14	0.003451
7	66.4247	(200)	0.7971	1.4057	11.94	0.005296
8	67.9614	(112)	0.5372	1.3776	17.88	0.003466
9	69.0937	(201)	0.6585	1.3578	14.68	0.004160
Average					~20nm	0.004059

Citation: Chauhan J, Shrivastav N, Dugaya A, et al. Synthesis and characterization of Ni and Cu doped Zno. *MOJ Poly Sci.* 2017;1(1):26–34.
DOI: 10.15406/mojps.2017.01.00005

Table 3 XRD Analysis of ZnO: Cu

Peak No.	2θ (degree)	hkl	FWHM (β)	d(A°)	D(nm)	ε
1	31.7477	(100)	0.2310	2.8151	35.84	0.003533
2	34.4167	(002)	0.2021	2.6026	41.26	0.002838
3	36.2567	(101)	0.2339	2.4747	35.82	0.003107
4	47.5196	(102)	0.2888	1.9111	30.13	0.002853
5	56.5970	(110)	0.3177	1.6242	28.47	0.002566
6	62.8860	(103)	0.3465	1.4765	26.94	0.002466
7	66.4044	(200)	0.4476	1.4061	21.26	0.002975
8	67.9411	(112)	0.3813	1.3780	28.18	0.002461
9	69.0532	(201)	0.3812	1.3585	25.36	0.002410
Average					~30nm	0.002801

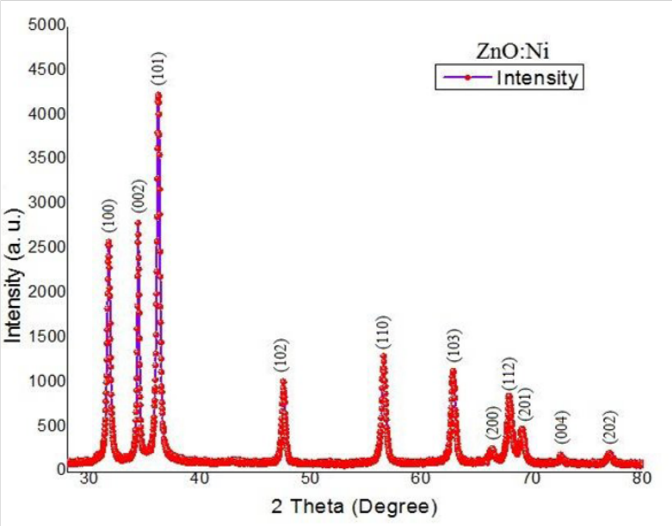

Figure 6 XRD Pattern of ZnO:Ni.

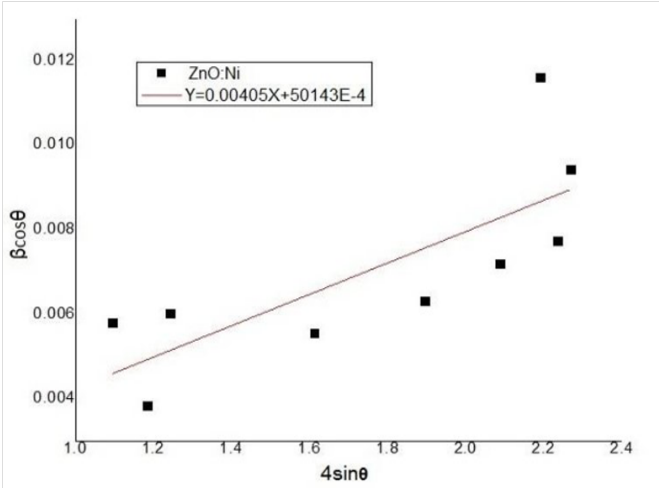

Figure 7 W-H Plot of ZnO:Ni.

The photoluminescence originates from the recombination of surface states. The photoluminescence spectra over wavelength range 350-900nm observed.[18] The photoluminescence profile given in the Figure 10 deal with the emission spectrum of undoped ZnO, Ni doped ZnO and Cu doped ZnO with an excitation wavelength of 395nm. PL spectra of undoped ZnO have highest intensity at the wavelength of 468.135nm which is corresponds to blue emission of visible spectrum which is arises due to surface defects which may come during the grinding process of sintered sample and one other peak in red band. The spectrum exhibits two emission peaks, one is located at around (468.13nm, 410.79nm and 411.79nm for undoped ZnO, ZnO: Ni and ZnO: Cu respectively) (UV region) corresponding to the near band gap excitonic emission[19] and the other is located at around 710 nm attributed to the presence of singly ionized oxygen vacancies.[20]

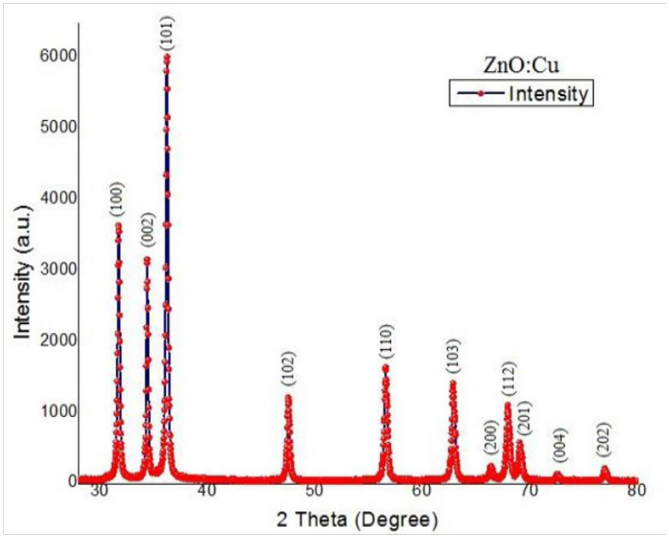

Figure 8 XRD Pattern of ZnO:Cu.

The emission is caused by the radiative recombination of a photo generated hole with an electron occupying the oxygen vacancy 45. Different level of bonding due to different materials (carrier) incorporation in the transition process is the main reason for different peaks. Generally oxide bond related peak shows in addition to main transition. We can calculate optical band gap of the material by using PL spectra. We have used formula-Where h is the plank constant that is 6.6260×10-34 Joule, C is the speed of light 3×1010m/sec and λ is the wavelength. By using this formula we found band gaps are 2.65eV, 3.02eV and 3.01Ev of undoped ZnO, Ni doped ZnO and Cu doped ZnO respectively.

Citation: Chauhan J, Shrivastav N, Dugaya A, et al. Synthesis and characterization of Ni and Cu doped Zno. *MOJ Poly Sci.* 2017;1(1):26–34.
DOI: 10.15406/mojps.2017.01.00005

The FTIR spectrum of Undoped ZnO, Ni doped ZnO and Cu doped ZnO at room temperature is shown in Figure 11. These spectrum shows the IR absorption due to the various vibration modes. The series of absorption in the current FTIR Spectra correspond to the impurities present in the samples. The peak at 667cm^{-1} is attributed to O=C=O bending vibration. The band in the region 670-1000cm^{-1} is due to =C-H bending of alkene while at 1660cm-1 is due C=C stretch of the same. The prominent peaks at 1071cm^{-1} and 1156cm^{-1} are because of C-O stretch (alcohol). The absorption bands observed around 1280cm^{-1} and 1330cm^{-1} correspond to C-O stretching (acid). The peaks around 1383cm^{-1} and 1460cm^{-1} reveal the presence of –C-H bending vibration of alkane and that around 2850-3000cm^{-1} reveal its C-H stretching vibrations. The broad absorption band in the region of 3400cm^{-1} corresponds to the O-H stretching vibrations of water present in the powder sample UV-Vis spectra are observed in the 200-800nm range. The prepared samples were first dispersed in water Before the UV Characterization we have dissolve 10mg of each sample in the 50ml DI separately to form a monodispersed solution. After this each sample was sonicated for 30 min.

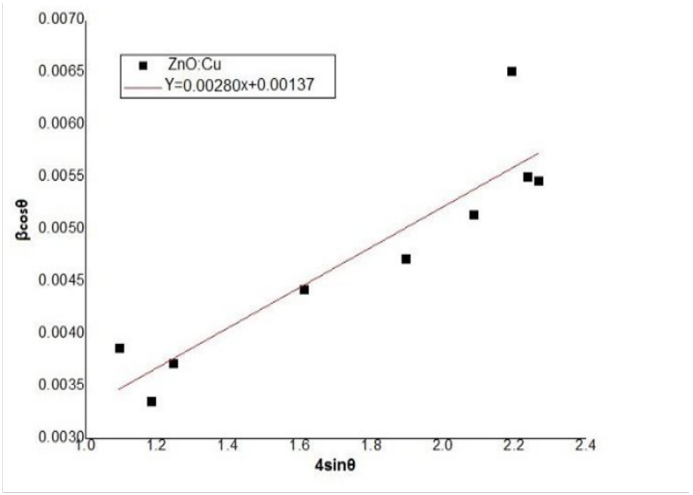

Figure 9 W-H Plot of ZnO:Cu.

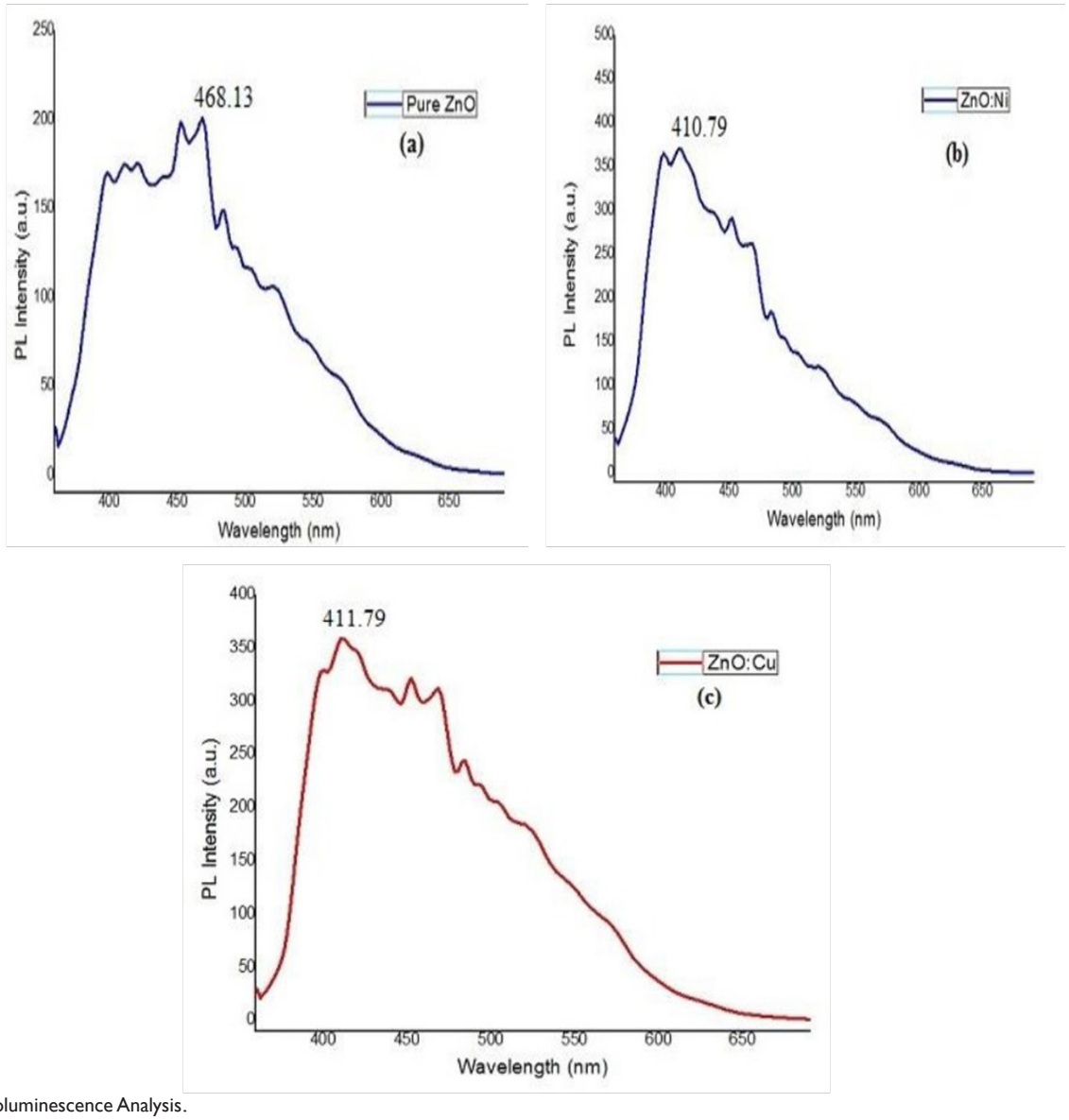

Figure 10 Photoluminescence Analysis.

Citation: Chauhan J, Shrivastav N, Dugaya A, et al. Synthesis and characterization of Ni and Cu doped Zno. *MOJ Poly Sci.* 2017;1(1):26–34. DOI: 10.15406/mojps.2017.01.00005

All three samples are not having any peak in the visible region. Optical absorption of Un doped, Nickel doped ZnO and Copper Doped ZnO are shown in Figure 12 the absorption spectra of un doped ZnO, ZnO:Ni and ZnO:Cu lie at 372nm, 376 and 380nm, respectively. The band gap values corresponding to these maxima are 3.33eV, 3.30eV and 3.26eV, respectively. These values are obviously red-shifted with respect to the band gap of undoped as well as bulk ZnO (3.37 eV).

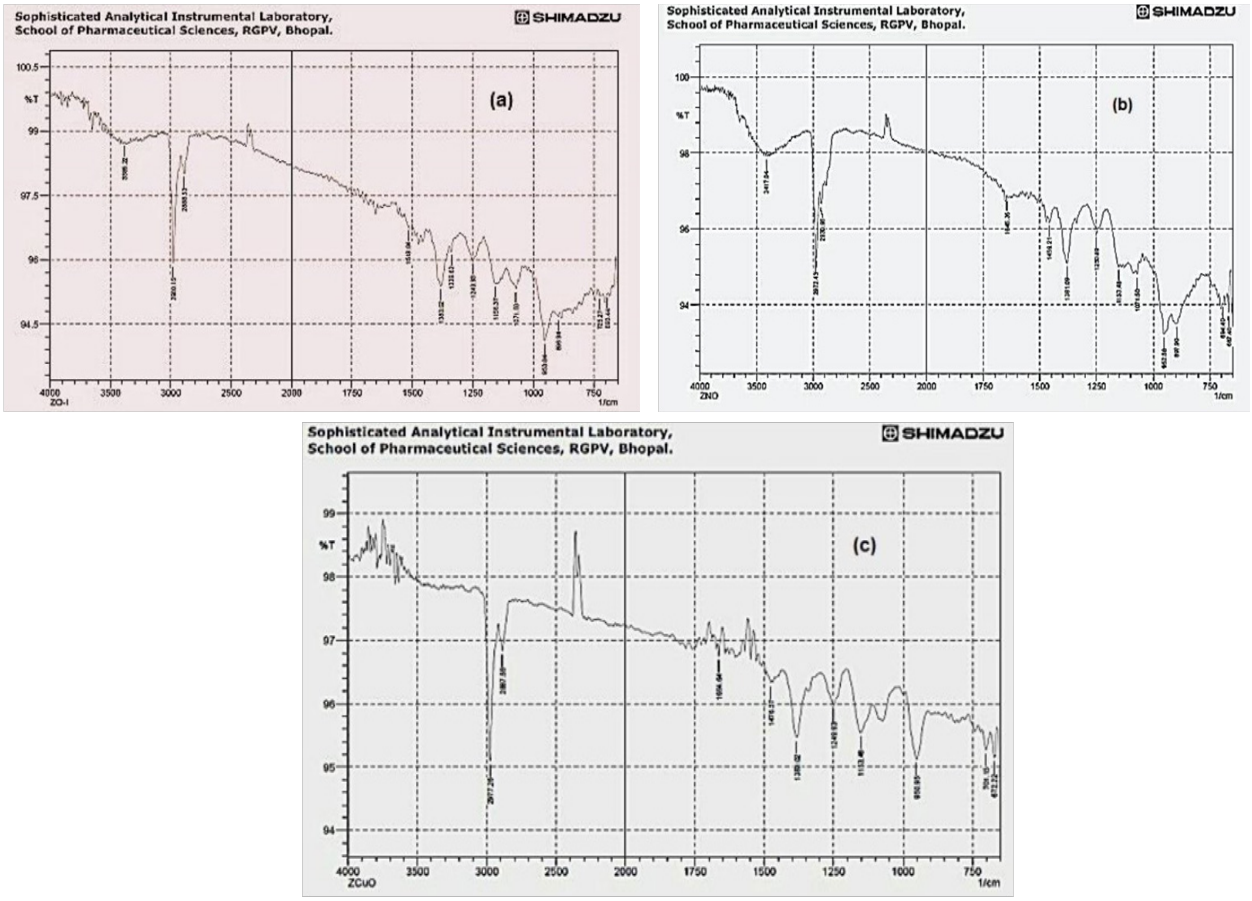

Figure 11 FTIR Pattern of (a) Undoped ZnO, (b) ZnO:Ni, (c) ZnO:Cu.

Table 4 XRD Analysis of samples corresponding to Peak (101)

Sample	2θ (degree)	FWHM (β)	Grain size(nm)	Avg. Strain(x 10^{-3})	Non uniform strain(x 10^{-5})
ZnO	36.2365	0.3985	~21	5.297	-3.19
ZnO: Ni	36.2365	0.3639	~24	4.6	-6.89
ZnO: Cu	36.2567	0.2339	~36	3.1	-0.745

Table 5 Summary of characterization

Sample	XRD		Photoluminescence	UV-Vis	FTIR
	D(nm)	ε			
ZnO	~20	0.004235	Ip~468.13 (2.65 eV), blue	λ max= 372nm	O-H, C-H, -C-H, =C-H, C-O bands
ZnO: Ni	~22	0.004059	Ip~410.79 (3.02 eV), violet	λ max=376nm	O-H, -C-H, C-O, =C-H bands
ZnO: Cu	~30	0.002801	Ip~411.79 (3.01 eV), violet	λ max= 380nm	O-H, C-H, -C-H, =C-H, C-O bands

Citation: Chauhan J, Shrivastav N, Dugaya A, et al. Synthesis and characterization of Ni and Cu doped Zno. *MOJ Poly Sci.* 2017;1(1):26–34.
DOI: 10.15406/mojps.2017.01.00005

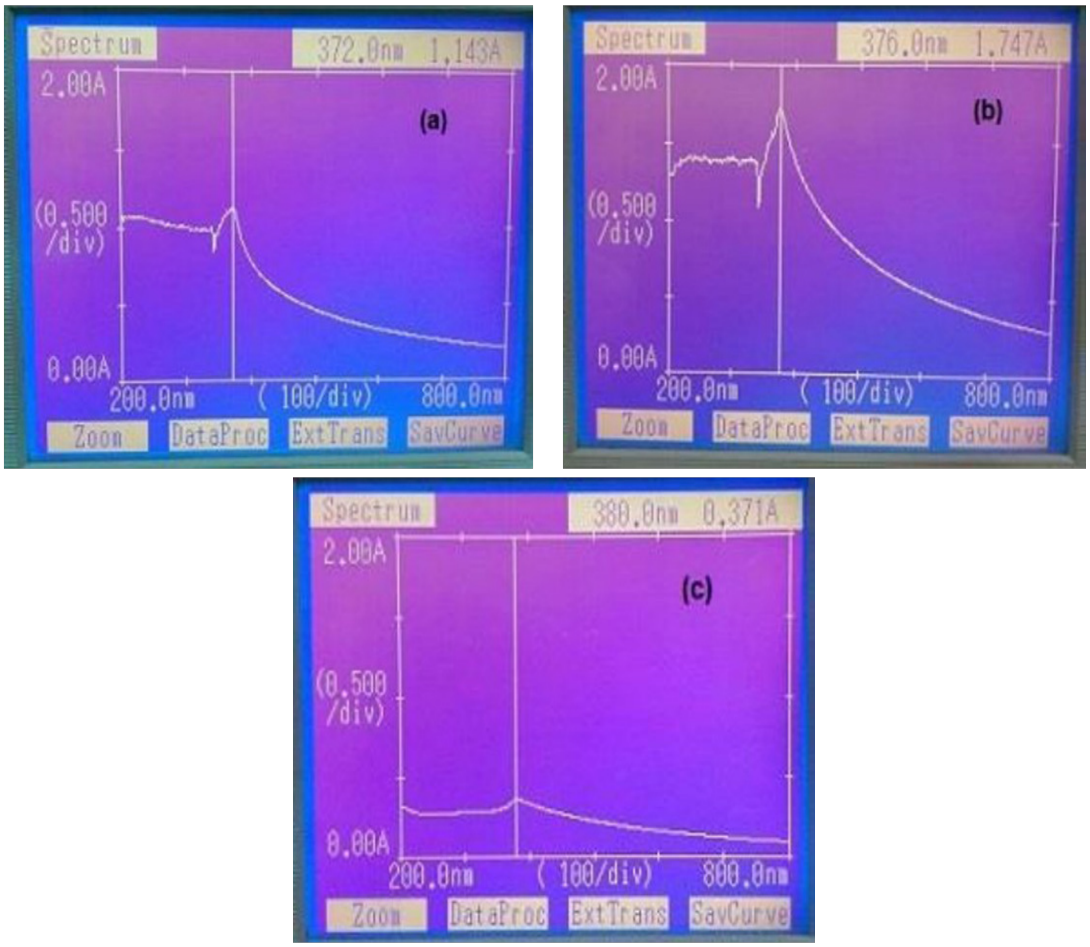

Figure 12 UV-Vis Spectra of (a) ZnO, (b) ZnO:Ni, (c) ZnO:Cu.

Conclusion

We have successfully synthesized samples using chemical co-precipitation method. UV-Vis absorption spectra revealed red shift compared to the undoped ZnO, The structural analysis clearly indicate that pure phase of ZnO, ZnO: Ni and ZnO: Cu are formed and all have wurtzite structural. XRD analysis confirmed that there is no any secondary phase formed it means that Ni_{2+} and Cu_{2+} replace the Zn_{2+} successfully in Ni doped ZnO and Cu doped ZnO respectively. Pure ZnO sample has the lowest grain size that is ~20nm, Ni doped and Cu doped ZnO have ~22nm and ~30nm respectively. Average strain is depends on the size of the particle as the size of the particle decrease strain is increases. PL spectra shows a blue shifting of peak wavelength from undoped ZnO to doped ZnO. Optical band gap is calculated using PL spectra and it was found 2.65eV, 3.02eV and 3.01eV of undoped ZnO, Ni doped ZnO and Cu doped ZnO respectively. Wavelength in UV-Vis spectra is shifted from lower to higher.

Acknowledgements

None.

Conflict of interest

The author declares no conflict of interest.

References

1. Eric Drexler K. *Engines of Creation: The Coming Era of Nanotechnology*. Doubleday; 1986. p. 1–10.
2. European Commission. The 7th frame program.
3. Meron T, Markovich G. Ferromagnetism in Colloidal Mn^{2+}- Doped ZnO Nanocrystals. *J Phys Chem B*. 2005;109(43):20232–20236.
4. Liang S, Sheng H, Liu Y, et al. ZnO #chottky ultraviolet photodetectors. *Journal of Crystal Growth*. 2001;225(2-4):110–113.
5. Shishiyanu ST, Shishiyanu TS, Lupan OI. Sensing characteristics of tin-doped ZnO thin films as NO_2 gas sensor. *Sensors and Actuators B*. 2005;107:379–386.
6. Huang MH, Mao S, Feick H, et al. Room-temperature ultraviolet nanowire nanolasers. *Science*. 2001;292(5523):1897–1899.
7. Saito N, Haneda H, Sekiguchi T, et al. Low-temperature fabrication of light-emitting zinc oxide micropatterns using self-assembled monolayers. *Advanced Materials*. 2002;14(6):418–421.
8. Ma Y, Ricciuti C, Miller T, et al. Enhanced catalytic combustion using sub-micrometer and nano-size platinum particles. *Energy Fuels*. 2008;22(6):3695–3700.
9. Segets D, Gradl J, Taylor RK, et al. Analysis of optical absorbance spectra for the determination of ZnO nanoparticle size distribution, solubility, and surface energy. *ACS Nano*. 2009;3(7):1703–1710.

Citation: Chauhan J, Shrivastav N, Dugaya A, et al. Synthesis and characterization of Ni and Cu doped Zno. *MOJ Poly Sci.* 2017;1(1):26–34.
DOI: 10.15406/mojps.2017.01.00005

10. Chaari M, Matoussi A. Electrical conduction and dielectric studies of ZnO pellets. *Physica B: Physics of Condensed Matter*. 2012;407(17):3441–3447.

11. Corso AD, Posternak M, Resta R, et al. Ab initio study of piezoelectricity and spontaneous polarization in ZnO. *Physical Review B*. 1994;50(15):10715.

12. Wang ZL. Zinc oxide nanostructures: growth, properties and Applications. *Journal of Physics Condensed Matter*. 2004;16:R829–R858.

13. Becheri A, Durr, M, Nostro PL, et al. Synthesis and characterization of zinc oxide nanoparticles: application to textiles as UV-absorbers. *Journal of Nanoparticle Research*. 2008;10(4):679–689.

14. Schaller RD, Klimov VI. High efficiency carrier multiplication in PbSe nanocrystals: implications for solar energy conversion. *Physical Review Letters*. 2004;92:186601.

15. Liz-Marzan LM. Tailoring surface plasmons through the morphology and assembly of metal nanoparticles. *Langmuir*. 2006;22(1):32–41.

16. Rodrigues P, Caballero J, Villegas AC, et al. Controlled precipitation methods: formation mechanism of ZnO nanoparticles. *Journal of the European Ceramic Society*. 2001;21(7):925–930.

17. Bragg WH. *Phil Mag*. 1912;23:136.

18. Chauhan J, Pateria1 D. Synthesis, Characterization and thermoluminescence Studies of $(ZnS)_{1-x}(MnTe)_x$ nanophosphors. *American Journal of Nanomaterials*. 2016;4(3):52–57.

19. Williams G, Kamat PV. Graphene-semiconductor nanocomposites: excited-state interactions between ZnO nanoparticles and graphene oxide. *Langmuir*. 2009;25(24):13869–13873.

20. Huang MH, Wu Y, Feick H, et al. Catalytic growth of zinc oxide nanowires by vapor transport. *Advanced Materials*. 2001;13(2):113–116.

Citation: Chauhan J, Shrivastav N, Dugaya A, et al. Synthesis and characterization of Ni and Cu doped Zno. *MOJ Poly Sci.* 2017;1(1):26–34.
DOI: 10.15406/mojps.2017.01.00005